Amphiregulin mediates non-cell-autonomous effect of senescence on reprogramming

Mathieu von Joest[1,3], Cheng Chen[1], Thibaut Douché[2], Aurelie Chiche[1], Mariette Matondo[2], Han Li[1*]

[1] *Cellular Plasticity & Disease Modelling,*

Dept. of Developmental & Stem Cell Biology, CNRS UMR 3738

[2] *Proteomics Platform, Mass Spectrometry for Biology Unit (MSBio), USR CNRS 2000,*

Institut Pasteur, 25 rue du Dr Roux, Paris 75015, France

[3] *Current address*: *Laboratory of chromatin and gene regulation during development, Imagine Institute, INSERM UMR1163, 75015, Paris, France*

* *Correspondence*: Han Li

Institut Pasteur,

25 rue du Dr Roux, Paris 75015, France

Tel: +33 (0)1 45 68 8484

Fax: +33 (0)1 45 68 8963

Email: han.li@pasteur.fr

Key words: cellular senescence / SASP/ in vitro & in vivo reprogramming / cellular plasticity / amphiregulin

Running title: Senescence-associated amphiregulin modulates reprogramming

Cellular senescence is an irreversible growth arrest with a highly dynamic secretome, termed the senescence-associated secretory phenotype (SASP). Senescence has been implicated in somatic reprogramming to pluripotency. The cell-intrinsic proliferation arrest is a barrier for reprogramming, whereas the SASP facilitates the cell fate conversion in nonsenescent cells. However, the mechanisms by which reprogramming-induced senescence regulates cell plasticity are not well understood. Here, we have further investigated how the heterogeneity of paracrine senescence impacts reprogramming. We show that senescence promotes *in vitro* reprogramming in a stress-dependent manner. We identified a catalog of SASP factors and pathways potentially involved in the cell fate conversion using an unbiased proteomic analysis. Amphiregulin (AREG), a growth factor frequently secreted by the senescent cells, promotes *in vitro* reprogramming by

accelerating proliferation and MET via the EGFR signaling pathway. Of note, AREG treatment diminished the negative effect of donor age on reprogramming. Finally, AREG enhances *in vivo* reprogramming in the skeletal muscle. Hence, senescence could facilitate cellular plasticity via various SASP factors to promote reprogramming and tissue repair.

BACKGROUND

Cellular senescence is a stress response characterized by a permanent cell-cycle arrest, acquisition of a senescence-associated secretory phenotype (SASP), and resistance to apoptosis (Hernandez-Segura et al., 2018). Senescence is involved in variety biological and pathological processes including development, tissue repair, tumorigenesis, and organism aging (Munoz-Espin and Serrano, 2014; Rhinn et al., 2019). Of note, SASP plays a crucial role in mediating senescence non-cell autonomous functions by interacting with neighboring cells and the surrounding microenvironment (Ito et al., 2017). It is becoming clear that senescence phenotypes, particularly SASP composition, are highly heterogeneous and depending on the initial stimuli, the affected cell type, and the anatomic location (Hernandez-Segura et al., 2017) (Ito et al., 2017).

Cellular reprogramming is a process of converting fully differentiated cells back to the pluripotent state, which has tremendous potentials in many areas of biomedical research (Takahashi and Yamanaka, 2006; Robinton and Daley, 2012). Interestingly, recent studies revealed that senescence has both cell-autonomous and non-cell-autonomous effects on reprogramming (Aarts et al., 2017; Banito et al., 2009; Chiche et al., 2017; Mosteiro et al., 2016; Mosteiro et al., 2018). Ectopic expression of reprogramming factors: Oct4, Klf4, Sox2, and c-Myc (OSKM), induced senescence as a cell intrinsic barrier for reprogramming (Banito et al., 2009), which in turn promote cellular plasticity and reprogramming in the non-senescent cells via SASP, in particularly by interleukin-6 (IL-6) (Chiche et al., 2017; Mosteiro et al., 2016; Mosteiro et al., 2018). However, the mechanisms by which paracrine senescence, with specific SASP factor(s), regulate cellular plasticity in the context of reprogramming remain not fully understood.

The epidermal growth factor receptor (EGFR) signaling pathway is one of the most important pathways that regulate cellular growth, proliferation, differentiation, and survival (Herbst, 2004). Although it is important for embryonic stem cells functions (Schuldiner et al., 2000; Yu et al., 2019) and the early embryonic development (Kim et al., 1999), the role of the EGFR signaling pathway in somatic reprogramming remains poorly understood. A variety of senescent cells produce abundant amphiregulin (AREG) (Coppe et al., 2010), a low-affinity EGFR ligand (Jones et al., 1999; Shoyab et al., 1988). Of note, accumulating evidence indicates AREG is a vital mediator of the immune response in infection and tissue repair (Zaiss et al., 2015). It has been suggested that AREG regulates senescence (Pommer et al., 2021) and contributes to an immunosuppressive tumor microenvironment (Xu et al., 2019). Given

74 the pleiotropic functions of AREG, its roles in mediating senescence functions remain largely
75 unexplored.
76
77 In this study, we investigated how paracrine senescence impacts reprogramming focusing on the stress
78 dependent SASP heterogeneity and identified a collection of SASP factors potentially important for
79 cellular plasticity using unbiased proteomic analysis. Next, we demonstrated that AREG enhances
80 reprogramming both *in vitro* and *in vivo* via EGFR and alleviates the age-associated reduction in
81 reprogramming.
82
83 **RESULTS**
84 **Paracrine senescence promotes *in vitro* reprogramming in a stress-dependent manner**
85 Given senescence can impact reprogramming in both cell-autonomous and non-cell-autonomous
86 manner (Chiche et al., 2020), and SASP composition is highly context-dependent, determined by both
87 the initial stress and the tissue/cell of origin(Hernandez-Segura et al., 2017; Ito et al., 2017). We
88 reasoned stress dependent SASP might impact reprogramming efficiency differently. To address this
89 question, we treated non-reprogrammable wild-type (WT) primary mouse embryonic fibroblasts (MEFs)
90 with three different stimuli (replicative senescence (RS), γ-irradiation (IRIS), and oncogene-induced
91 senescence (OIS)) to induce senescence and generate distinct SASP (Figure S1A). Meanwhile, we used
92 the MEFs generated from a previously established reprogrammable mouse model (i4F) (Abad et al.,
93 2013). The reprogramming was induced by adding doxycycline (DOX) in i4F-MEFs either co-cultured
94 with the senescent WT MEFs (co-culture) or cultured directly with the senescence conditioned medium
95 (CM) according to the experimental scheme illustrated (Figure 1A). After 12 days DOX treatment,
96 induced pluripotent stem cells (iPSCs) colonies were stained using alkaline phosphatase (AP) to
97 determine the reprogramming efficiency. For the co-culture system, i4F MEFs were seeded on top of
98 $2x10^5$ WT MEFs (either control or OIS treated) with various ratios of 1:3, 1:5, and 1:10 (i4F: WT), to
99 determine the optimal experimental condition. We found the reprogramming efficiency increased the
100 most in the ratio of 1:10 (i4F: WT) (Figure S1B). Next, we compared the relative reprogramming
101 efficiency of i4F MEFs and found that in both systems all stimuli can increase reprogramming efficiency
102 ranging from RS the least to OIS the most, except the positive effect of RS is diminished in the CM
103 system (Figure 1B & Figure 1C).
104
105 Reprogramming is a stepwise process with distinct phases: initiation, maturation, and stabilization
106 (Samavarchi-Tehrani et al., 2010). To determine at which stage the SASP exposure is most important
107 for enhancing reprogramming, we cultured i4F with either OIS-CM or Ctrl-CM in different order
108 (Figure 1D & Figure S1C). Culturing i4F-MEFs with OIS-CM for the first three days was sufficient to
109 induce the highest fold increase in reprogramming (Figure 1D). Conversely, initiating reprogramming
110 with Ctrl-CM for three days and replaced by OIS-CM completely abolished the beneficial effect (Figure

111 S1C). Active cell proliferation is rate-limiting for successful reprogramming (Ruiz et al., 2011), and
112 senescent cells secrete various growth factors (Coppe et al., 2010). Therefore, we compared the growth
113 properties of i4F MEFs cultured with either OIS-CM or Ctrl-CM over 12 days in the absence of DOX.
114 The bromodeoxyuridine (BrdU) incorporation rates after 72 hours were similar between Ctrl and OIS
115 (Figure S1E). However, the accumulative growth curve indicated that i4F MEFs grew faster in OIS-CM
116 than in Ctrl-CM (Figure S1D). Hence, certain SASP factors promote *in vitro* reprogramming transiently
117 at the initiation phase of reprogramming, which partially correlates with an enhanced proliferation rate.
118

119 **Conditioned medium of OIS-Il6$^{-/-}$ promoted reprogramming efficiently**

120 We sought to identify SASP factors responsible for the stress-dependent effect on reprogramming.
121 Given that IL-6 signaling is required for *in vitro* reprogramming (Brady et al., 2013; Mai et al., 2018),
122 and IL-6 is a crucial mediator of the senescence paracrine signals in promoting *in vivo* reprogramming
123 (Chiche et al., 2017; Mosteiro et al., 2016; Mosteiro et al., 2018), we determined firstly the effect of CM
124 of senescent MEFs derived from *Il6*$^{-/-}$ mice on reprogramming. Of note, IL-6 plays a critical role in
125 mediating OIS, and reduction of IL-6 via RNA interference efficiently bypassed OIS in human diploid
126 fibroblasts (Kuilman et al., 2008). Interestingly, we found *Il6*$^{-/-}$ MEF entered senescence efficiently upon
127 OIS, judging by both senescence-associated beta-galactosidase (SAβGal) staining (data not shown) and
128 qPCR (Figure S2A). Surprisingly, CM generated from senescent *Il6*$^{-/-}$ MEFs by IRIS or OIS enhanced
129 reprogramming efficiency to a similar level as WT (Figure 2A). To ensure the observed enhancement is
130 IL-6 independent, we compared the IL-6 level in the OIS-CMs of both WT and *Il6*$^{-/-}$ by ELISA. In WT,
131 IL-6 is significantly increased in the OIS-CM compared to Ctrl-CM. While, IL-6 is non-detectable in
132 both Ctrl-CM and OIS-CM of *Il6*$^{-/-}$ (Figure S2B). Of note, IL-6 neutralizing antibody could potently
133 repress the increased reprogramming efficiency only in the CM-WT but failed to do so in the CM-*Il6*$^{-/-}$
134 (Figure 2B and Figure S2C). Thus, there are SASP factors other than IL-6 that can robustly promote *in*
135 *vitro* reprogramming.
136

137 ***In vivo* reprogramming in the skeletal muscle is not affected by IL6 deficiency**

138 We reported previously that injury-induced senescence enabled reprogramming in the skeletal muscle
139 (Chiche et al., 2017). We wondered whether tissue injury could induce reprogramming in the skeletal
140 muscle of *Il6*$^{-/-}$ mice. To test this, we generated *Il6*$^{-/-}$;i4F mouse model and injured the Tibialis anterior
141 (TA) muscle of both *Il6*$^{+/-}$;i4F and *Il6*$^{-/-}$;i4F mice with the snake venom cardiotoxin (CTX). In the same
142 time, we added doxycycline (dox) in the drinking water for 7 days to induce *in vivo* reprogramming and
143 TAs were collected at 10 days post-injury (DPI) as previously described (Chiche et al., 2017). The
144 expression of the OSKM triggered extensive dysplasia and reprogramming (Nanog^{+} cells) in the injured
145 TA of male i4F mice (Figure 2C and Figure S2D). Consistent with a previous report (Mosteiro et al.,
146 2018), the reprogramming was significantly reduced in the females i4F mice comparing to male i4F
147 mice (Figure 2C & 2D,0 Figure S2D). Interestingly, *Il6*$^{-/-}$; i4F mice exhibited a similar level of dysplasia

148 and Nanog^{+} cells as the sex-matched *Il6*$^{+/-}$;i4F mice (Figure 2C & 2D, Figure S2D). Besides, we did not
149 observe a difference in the senescence induction in males regardless of the genotype (Figure S2E &
150 S2F). Thus, *in vivo* reprogramming in the skeletal muscle is not impaired in the IL-6 deficient
151 reprogrammable mice.
152
153 **Soluble factor fraction of the CM-OIS mediates *in vitro* reprogramming**
154 To gain a comprehensive profile of the SASP heterogenous composition, we determined firstly the effect
155 of different fractions of CM on reprogramming, which could facilitate reprogramming due to secreted
156 proteins, extracellular vesicles, or small-molecule metabolites. We examined whether the boiled CM
157 could promote *in vitro* reprogramming since boiling denatures most proteins without affecting small
158 molecule metabolites, and found that boiled CM completely abolished *in vitro* reprogramming,
159 indicating that secreted proteins are crucial in promoting reprogramming (Figure S3A).
160
161 Exosomes are small extracellular vesicles (sEV) released from almost all cell types and are critical
162 mediators of intercellular communication (Kalluri and LeBleu, 2020). Increasing evidence suggests that
163 senescent cells secret exosomes with distinct features, contributing to paracrine senescence (Borghesan
164 et al., 2019). To examine whether senescence-associated exosomes regulate *in vitro* reprogramming, we
165 isolated sEV and supernatants (SN) fractions from Ctrl-CM and OIS-CM using serial ultracentrifugation
166 and filtering with a 0.22-µm filter (Thery et al., 2006). Both OIS-sEV and Ctrl-sEV were suspended in
167 Ctrl-SN to determine whether they can drive paracrine senescence. Consistent with the previous report
168 (Borghesan et al., 2019), the OIS-sEV in Ctrl-SN induces several senescence markers in i4F MEFs, as
169 shown by a decrease in BrdU incorporation and an increase in mRNA expression of p16 and ARF
170 (Figure S3B & Figure S3C). Next, we wondered whether OIS-sEV could also affect reprogramming.
171 Comparing to Ctrl-SN, the OIS-SN significantly enhanced the reprogramming efficiency to a similar
172 level as OIS-CM (Figure 3A). However, OIS-sEV in Ctrl-SN exhibited a much lower reprogramming
173 efficiency than OIS-SN, similarly to Ctrl-sEV in Ctrl-SN (Figure 3A). Hence, the soluble fraction of
174 OIS-CM is essential for promoting in vitro reprogramming.
175
176 **Quantitative proteomics analysis of SASP composition**
177 To gain a comprehensive profile of the heterogenous SASP composition and maximize the detection of
178 SASP factors important for reprogramming other than IL6, we isolated the soluble protein fractions
179 from the OIS-CM and Ctrl-CM of *Il6*$^{-/-}$ MEFs to perform quantitative proteomic analysis. The label-free
180 data-independent acquisition (DIA) tandem mass spectrometry strategy allows sensitive and unbiased
181 detection of SASP proteins in a reproducible manner (Basisty et al., 2020; Gillet et al., 2012). To ensure
182 the correct identification, we only included a protein when it can be detected in all six replicates of one
183 condition. The proteomic analysis identified a total of 1955 proteins in both conditions, including 249
184 proteins with a significant differential expression (q-value <0.01) that had a fold change of at least 2-

185 fold (SEN/CTL) (Figure 3B). Of note, 217 proteins were exclusively detected in one condition (185 in
186 SEN and 32 in CTL) (Figure 3C), which were assumed differentially abundant between the conditions
187 and included in the data analysis. We found many known SASP factors are more abundantly secreted in
188 the OIS-SN, such as SPP1, PLAU, and MMP3 (Figure S3D). Of note, we did not detect IL-6 in both
189 conditions. Interestingly, there is less than 50% overlap between our study and a recent large-scale
190 human SASP proteomic study (human fibroblast-OIS, 115/386), suggesting heterogenous in SASP
191 composition between species (Hernandez-Segura et al., 2017).
192
193 To identify which biological pathways/responses are mediated by SASP factors, we performed pathway
194 and network analyses on the proteins that are either more abundantly or exclusively secreted from the
195 SEN condition. We found the most dominant clusters of gene ontology (GO) pathways are related to
196 morphogenesis and stress response, including cell morphogenesis in development and differentiation,
197 response to growth factor, wounding response, and angiogenesis (Figure 3D). Besides, the hallmark
198 gene set enrichment analysis (GSEA) revealed several pathways that are associated with paracrine
199 senescence, including Epithelial-to-Mesenchymal transition (EMT) (Ansieau et al., 2008), TNFα
200 signaling via NFκB, inflammatory response, and p53 pathway (Coppe et al., 2010) (Figure S3E).
201
202 **Amphiregulin enhances *in vitro* reprogramming efficiency and kinetic**
203 Of note, several pathways identified by the bioinformatic analysis are also important for somatic
204 reprogramming, such as EMT (Liu et al., 2013), apoptosis (Kawamura et al., 2009; Kim et al., 2018),
205 hypoxia (Yoshida et al., 2009), and p53 pathway (Hong et al., 2009; Kawamura et al., 2009; Marion et
206 al., 2009; Utikal et al., 2009). Given Mesenchymal-to-Epithelial transition (MET) is required in the
207 initiation phase of *in vitro* reprogramming (Li et al., 2010; Liu et al., 2013; Samavarchi-Tehrani et al.,
208 2010), and because our data suggested that paracrine senescence promotes reprogramming at the early
209 stage (Figure 1D), we investigated the proteins overlapped with the EMT gene set and found many
210 factors crucial for *in vitro* reprogramming, such as BMP1 and TGFβ (Li et al., 2010; Liu et al., 2013;
211 Samavarchi-Tehrani et al., 2010)(Figure S4A).
212
213 AREG is an EGFR ligand (Shoyab et al., 1989) and has diverse functions in development, tissue
214 regeneration, and tumorigenesis (Zaiss et al., 2015). Since both OIS and muscle injury strongly induce
215 AREG (Burzyn et al., 2013; Pommer et al., 2021), we wondered whether AREG could partially mediate
216 the effect of paracrine senescence on reprogramming both *in vitro* and *in vivo*. Interestingly, AREG is
217 the only EGFR ligand that has significantly increased mRNA expression in OIS comparing to IRIS
218 (Figure S4B). To formally test the effect of AREG on reprogramming, we added different concentrations
219 of the recombinant AREG protein for the first three days during reprogramming, consistent with the CM
220 experiment (Figure 1D). AREG treatment enhanced reprogramming efficiency in a dosage-dependent

221 manner (Figure 4A). We next removed DOX at different time points to examine the ability of AREG to
222 facilitate OSKM transgene-independent clonal growth, a hallmark of iPSCs. AREG treatment yielded
223 iPSCs clones after only 5 days of OSKM expression, compared to 8 days in the control condition (Figure
224 4B), suggesting a faster reprogramming kinetic.
225
226 **AREG accelerates cell cycle and the process of MET during reprogramming**
227 We sought to understand the mechanism by which AREG promotes reprogramming. The reported role
228 of AREG in proliferation and EMT (Berasain and Avila, 2014) prompted us to analyze cell proliferation
229 and MET process, two vital cellular events that occurred in the early stage of reprogramming (Sancho-
230 Martinez and Izpisua Belmonte, 2013). We found that AREG treatment led to a larger fraction of cells
231 in S-phase and increased cell proliferation globally in MEFs alone (Figure S4C & S4D). Next, we
232 checked whether AREG affected MET during reprogramming by measuring the expression of several
233 mesenchymal and epithelial cell markers at different time points throughout reprogramming using qPCR.
234 In control, the expression of the mesenchymal markers, Zeb1 and Zeb2, were transiently upregulated
235 and gradually suppressed afterward. Interestingly, these markers were suppressed throughout the
236 reprogramming process in AREG treated condition (Figure 4C). Conversely, the expression of the
237 epithelial markers, Occludin and E-Cadherin, was higher in samples treated with AREG than the control
238 (Figure 4D). Besides, the expression of all the pluripotency markers, endogenous Oct4, Sox2, Klf4,
239 Nanog, Lin28, and Esrrb, gradually increased and peaked at the last stage reprogramming in control.
240 While in AREG treated condition, endogenous Oct4 and Nanog expression sharply increased at 6 days
241 and reached the plateau earlier than in the control (Figure 4E). However, the expression dynamic of
242 other pluripotent markers remained the same (Figure S4D), suggesting an action upon Nanog and Oct4
243 specifically rather than a mere reflection of the accelerated reprogramming. Taken together, these results
244 indicate that AREG enhances the efficiency and kinetic of reprogramming by increasing proliferation
245 rates and facilitating MET process.
246
247 **EGFR signaling pathway is important for reprogramming**
248 Since AREG is an atypical EGFR ligand (Zaiss et al., 2015), we wondered whether other EGFR ligands
249 could also promote somatic reprogramming and found that additional epidermal growth factor (EGF)
250 also improved the reprogramming efficiency (Figure 5A). Next, we examined whether EGFR activation
251 is necessary for the enhancement. AREG and Dox combination strongly induced the activation of EGFR
252 comparing to Dox alone or untreated control determined by the level of the phosphorylated EGFR using
253 Western blotting (Figure S5A). Besides, Lapatinib, a dual tyrosine kinase inhibitor of EGFR and human
254 epidermal growth factor receptor-2 (HER2) (Wood et al., 2004), canceled the effect of AREG on
255 reprogramming (Figure 5B and Figure S5A). Of note, a high concentration of Lapatinib alone
256 significantly repressed reprogramming (Figure S5B), suggesting EGFR signaling pathway might be
257 required for reprogramming. Hence, AREG promotes reprogramming in an EGFR dependent manner.

258

259 **AREG rescues age-dependent reduction in reprogramming**

260 Previously, we reported that murine dermal fibroblasts (MDFs) derived from old (> 2 years) mice had a
261 significant reduction in reprogramming efficiency comparing to MDFs derived from young (2 months)
262 mice (Li et al., 2009). Because AREG induces cell proliferation, we investigated whether AREG can
263 improve reprogramming in this context. Consistent with the previous report, MDFs from old (> 2 years)
264 i4F mice had much lower reprogramming efficiency comparing to MDFs from young (2 months) i4F
265 mice (Figure 5C). Notably, the addition of AREG to the aged MDFs rescued their low reprogramming
266 efficiency to the same level as the young MDFs (Figure 5C).

267

268 **AREG promotes *in vivo* reprogramming in the skeletal muscle**

269 It has been reported that AREG enhances the myogenic differentiation of skeletal muscle stem cells
270 (MuSCs) *in vitro* and facilitates muscle regeneration (Burzyn et al., 2013). We previously reported that
271 MuSC is a cell of origin for *in vivo* reprogramming (Chiche et al., 2017). Therefore, we hypothesize that
272 AREG might also improve *in vivo* reprogramming in the injured muscle. To address this question, we
273 administered AREG to the CTX-injured, DOX-treated male i4F mice according to the experimental
274 scheme illustrated in Figure 5D and evaluated reprogramming and senescence induction at 10 DPI.
275 (Note that the initial AREG injection was done i.m. as previously described (Burzyn et al., 2013).) There
276 were many more Nanog+ cells in the TA sections from mice treated with AREG comparing to the
277 control group (Figure 5E and Figure 5F). Conversely, there is no apparent difference in senescence
278 induction, detected by SAβGal staining (Figure 5E and Figure 5F). Because AREG was administrated
279 mainly i.p., we wondered whether it could also improve reprogramming in other tissues. Interestingly,
280 we also observed more Nanog+ cells in both pancreas and kidney, but not in the liver (Figure S5C),
281 suggesting a tissue-specific effect of AREG on *in vivo* reprogramming.

282

283 **Discussion:**

284 Here, we report that the impact of paracrine senescence on reprogramming is stress-dependent. The
285 quantitative proteomic analysis on the senescence-associated secretome identified a catalog of factors
286 involved in various biological processes that could potentially impact cell plasticity. We demonstrated
287 that the AREG enhances *in vitro* reprogramming efficiency and kinetic, at least in part, by accelerating
288 somatic cell proliferation and the process of MET. Of note, AREG treatment rescue the age-associated
289 reduction in reprogramming and facilitate *in vivo* reprogramming in a tissue-specific manner.

290

291 IL-6 is required for oncogene-induced senescence (Kuilman et al., 2008). Surprisingly, we could
292 efficiently induce senescence in *Il6*$^{-/-}$ MEFs (Figure S2A)(Kopf et al., 1994). Both ELISA and proteomic
293 analysis failed to detect IL-6 in the CM-OIS-*Il6*$^{-/-}$ (Figure S2B and Figure S2C), indicating that OIS-*Il6*$^{-}$
294 $^{/-}$ does not secrete IL-6. Thus, the discrepancy might be due to the compensation effect of germline

295 knockout, which often yields much weaker phenotypes than acute disruption of gene function (Housden
296 et al., 2017). Importantly, IL-6 blocking antibody did not abolish the beneficial effect of CM-OIS-*Il6*$^{-/-}$
297 on *in vitro* reprogramming (Figure 2B), highlighting the involvement of other SASP factors.
298
299 Consistently, we found that IL-6 deficiency supports *in vivo* reprogramming in the muscle (Figure 2C
300 and Figure 2D). Together with others, we have previously demonstrated that tissue injury-induced
301 senescence facilitates *in vivo* reprogramming in a paracrine manner, particularly by IL-6 (Chiche et al.,
302 2017; Mosteiro et al., 2016). A recent study reported a reduction of reprogramming in the pancreas of
303 i4F; *Il6*$^{-/-}$ mice (Mosteiro et al., 2018). Firstly, reprogramming-induced and injury-induced senescence
304 might produce different factors (Chiche et al., 2017; Mosteiro et al., 2018). Besides, IL-6 is a myokine
305 vital for muscle formation and growth (Serrano et al., 2008). Although many different cell types produce
306 IL-6 upon muscle injury, including macrophages and muscle stem cells (Munoz-Canoves et al., 2013),
307 muscle regeneration is only mildly affected in *Il6*$^{-/-}$ mice (Zhang et al., 2013), suggesting a potential
308 compensation by other members of the IL-6 cytokine family. Therefore, the tissue-specific requirement
309 of IL-6 for *in vivo* reprogramming might be due to distinct stress/tissue-dependent senescence secretome
310 and the pleiotropic functions of IL-6.
311
312 To gain an extensive and quantitative view on SASP factors, we performed an unbiased proteomic study
313 using CM-OIS-*Il6*$^{-/-}$ (Figure 3B). The bioinformatic network analysis revealed pathways predominantly
314 related to morphogenesis and response to growth factors (Figure 3C), where EGFR signaling pathways
315 play crucial roles. Of note, we used OIS-MEFs as a proxy for senescence induced by OSKM over-
316 expression or muscle injury to identify SASP factors, which might not fully recapitulate the *in vivo*
317 scenario. Future investigation will further elucidate the context-dependent SASP heterogeneity.
318
319 To shed some light on SASP factors other than IL-6 and reprogramming, we investigated the role of
320 AREG in this process. We found that AREG treatment could notably increase *in vitro* reprogramming
321 efficiency (Figure 4A) and kinetic (Figure 4B). Next, we showed that AREG could accelerate cell
322 proliferation (Figure S4C) and suppress mesenchymal markers (Figure 4C), suggesting AREG might
323 affect several cellular events necessary for the initiation phase of reprogramming(Sancho-Martinez and
324 Izpisua Belmonte, 2013). Interestingly, we found AREG could alleviate the negative impact of age on
325 reprogramming (Figure 5B), providing a straightforward solution to improve iPS cell generation during
326 aging (Mahmoudi et al., 2019). Of note, AREG treatment failed to further enhance reprogramming to
327 the similar level as the young (Figure 5B), reflecting the attenuated EGFR signaling in the aged skin
328 fibroblasts as previously reported (Shiraha et al., 2000; Tran et al., 2003).
329
330 Furthermore, we showed that AREG promotes *in vivo* reprogramming in the muscle (Figure 5E & 5F).
331 It has been reported that EGFR regulates the asymmetrical division of MuSCs (Wang et al., 2019), and

332 AREG could facilitate the differentiation of MuSCs *in vitro* (Burzyn et al., 2013; Zaiss et al., 2015).
333 Therefore, AREG might directly promote the cell plasticity of MuSCs, a primary cell origin of
334 reprogramming in the muscle (Chiche et al., 2017). Interestingly, AREG also promoted reprogramming
335 in the pancreas and kidney but not in the liver (Figure S5C), highlighting a tissue-specific mode of action.
336 Of note, recent studies showed that cyclic expression of OSKM could enhance muscle regeneration
337 (Ocampo et al., 2016). Given senescence is important for optimal wound healing (Demaria et al., 2014)
338 and limb regeneration (Yun et al., 2015), future investigation is warranted to determine whether the
339 rejuvenation effect of partial reprogramming is partially mediated by senescence.
340
341 In summary, we dissected the impact of paracrine senescence on reprogramming and revealed the role
342 of the AREG-EGFR signaling pathway in reprogramming. These findings may have important
343 implications for understanding senescence's involvement in tissue repair and *in vivo* reprogramming.

Acknowledgements

We are indebted to Jun Zhang for his excellent technical support in image analysis. We are grateful to the Central Animal Facility, the Proteomic Platform, the Cytometry Platform, and the Bioinformatics and Biostatistics Hub of the Institut Pasteur. Work in the laboratory of H.L. was funded by Institut Pasteur, Centre National pour la Recherche Scientific and the Agence Nationale de la Recherche (Laboratoire d'Excellence Revive, Investissement d'Avenir; ANR-10-LABX- 73; ANR-16-CE13-0017). This work is also supported by Fondation ARC (PJA 20161205028). AC was funded by the postdoctoral fellowships from the Revive Consortium.

AUTHOR CONTRIBUTIONS

M.VJ performed most of the experimental work, contributed to experimental design, data analysis, and discussions. C.C made critical experimental contributions. AC contributed experimentally. T.D performed proteomic analysis and data acquisition. M.M supervised the proteomic analysis and data interpretation. H.L. supervised the study, designed the experimental plan, interpreted the data and wrote the manuscript. All authors discussed the results and commented on the manuscript. The authors declare no competing financial interests with this paper.

REFERENCE

Aarts, M., Georgilis, A., Beniazza, M., Beolchi, P., Banito, A., Carroll, T., Kulisic, M., Kaemena, D.F., Dharmalingam, G., Martin, N., *et al*. (2017). Coupling shRNA screens with single-cell RNA-seq identifies a dual role for mTOR in reprogramming-induced senescence. Genes Dev *31*, 2085-2098.
Ansieau, S., Bastid, J., Doreau, A., Morel, A.P., Bouchet, B.P., Thomas, C., Fauvet, F., Puisieux, I., Doglioni, C., Piccinin, S., *et al*. (2008). Induction of EMT by twist proteins as a collateral effect of tumor-promoting inactivation of premature senescence. Cancer Cell *14*, 79-89.
Banito, A., Rashid, S.T., Acosta, J.C., Li, S., Pereira, C.F., Geti, I., Pinho, S., Silva, J.C., Azuara, V., Walsh, M., *et al*. (2009). Senescence impairs successful reprogramming to pluripotent stem cells. Genes Dev *23*, 2134-2139.
Basisty, N., Kale, A., Jeon, O.H., Kuehnemann, C., Payne, T., Rao, C., Holtz, A., Shah, S., Sharma, V., Ferrucci, L., *et al*. (2020). A proteomic atlas of senescence-associated secretomes for aging biomarker development. PLoS Biol *18*, e3000599.
Berasain, C., and Avila, M.A. (2014). Amphiregulin. Semin Cell Dev Biol *28*, 31-41.
Bindea, G., Mlecnik, B., Hackl, H., Charoentong, P., Tosolini, M., Kirilovsky, A., Fridman, W.H., Pages, F., Trajanoski, Z., and Galon, J. (2009). ClueGO: a Cytoscape plug-in to decipher functionally grouped gene ontology and pathway annotation networks. Bioinformatics *25*, 1091-1093.
Borghesan, M., Fafian-Labora, J., Eleftheriadou, O., Carpintero-Fernandez, P., Paez-Ribes, M., Vizcay-Barrena, G., Swisa, A., Kolodkin-Gal, D., Ximenez-Embun, P., Lowe, R., *et al*. (2019). Small

Extracellular Vesicles Are Key Regulators of Non-cell Autonomous Intercellular Communication in Senescence via the Interferon Protein IFITM3. Cell Rep *27*, 3956-3971 e3956.
Brady, J.J., Li, M., Suthram, S., Jiang, H., Wong, W.H., and Blau, H.M. (2013). Early role for IL-6 signalling during generation of induced pluripotent stem cells revealed by heterokaryon RNA-Seq. Nat Cell Biol *15*, 1244-1252.
Burzyn, D., Kuswanto, W., Kolodin, D., Shadrach, J.L., Cerletti, M., Jang, Y., Sefik, E., Tan, T.G., Wagers, A.J., Benoist, C., *et al*. (2013). A special population of regulatory T cells potentiates muscle repair. Cell *155*, 1282-1295.
Chiche, A., Chen, C., and Li, H. (2020). The crosstalk between cellular reprogramming and senescence in aging and regeneration. Exp Gerontol *138*, 111005.
Chiche, A., Le Roux, I., von Joest, M., Sakai, H., Aguin, S.B., Cazin, C., Salam, R., Fiette, L., Alegria, O., Flamant, P., *et al*. (2017). Injury-Induced Senescence Enables In Vivo Reprogramming in Skeletal Muscle. Cell Stem Cell *20*, 407-414 e404.
Coppe, J.P., Desprez, P.Y., Krtolica, A., and Campisi, J. (2010). The senescence-associated secretory phenotype: the dark side of tumor suppression. Annu Rev Pathol *5*, 99-118.
Demaria, M., Ohtani, N., Youssef, S.A., Rodier, F., Toussaint, W., Mitchell, J.R., Laberge, R.M., Vijg, J., Van Steeg, H., Dolle, M.E., *et al*. (2014). An essential role for senescent cells in optimal wound healing through secretion of PDGF-AA. Dev Cell *31*, 722-733.
Gillet, L.C., Navarro, P., Tate, S., Rost, H., Selevsek, N., Reiter, L., Bonner, R., and Aebersold, R. (2012). Targeted data extraction of the MS/MS spectra generated by data-independent acquisition: a new concept for consistent and accurate proteome analysis. Mol Cell Proteomics *11*, O111 016717.
Herbst, R.S. (2004). Review of epidermal growth factor receptor biology. Int J Radiat Oncol Biol Phys *59*, 21-26.
Hernandez-Segura, A., de Jong, T.V., Melov, S., Guryev, V., Campisi, J., and Demaria, M. (2017). Unmasking Transcriptional Heterogeneity in Senescent Cells. Curr Biol *27*, 2652-2660 e2654.
Hernandez-Segura, A., Nehme, J., and Demaria, M. (2018). Hallmarks of Cellular Senescence. Trends Cell Biol *28*, 436-453.
Hong, H., Takahashi, K., Ichisaka, T., Aoi, T., Kanagawa, O., Nakagawa, M., Okita, K., and Yamanaka, S. (2009). Suppression of induced pluripotent stem cell generation by the p53-p21 pathway. Nature *460*, 1132-1135.
Housden, B.E., Muhar, M., Gemberling, M., Gersbach, C.A., Stainier, D.Y., Seydoux, G., Mohr, S.E., Zuber, J., and Perrimon, N. (2017). Loss-of-function genetic tools for animal models: cross-species and cross-platform differences. Nat Rev Genet *18*, 24-40.
Ito, Y., Hoare, M., and Narita, M. (2017). Spatial and Temporal Control of Senescence. Trends Cell Biol *27*, 820-832.
Jones, J.T., Akita, R.W., and Sliwkowski, M.X. (1999). Binding specificities and affinities of egf domains for ErbB receptors. FEBS Lett *447*, 227-231.
Kalluri, R., and LeBleu, V.S. (2020). The biology, function, and biomedical applications of exosomes. Science *367*.
Kawamura, T., Suzuki, J., Wang, Y.V., Menendez, S., Morera, L.B., Raya, A., Wahl, G.M., and Belmonte, J.C. (2009). Linking the p53 tumour suppressor pathway to somatic cell reprogramming. Nature *460*, 1140-1144.
Kim, C.H., Chae, H.D., Cheon, Y.P., Kang, B.M., Chang, Y.S., and Mok, J.E. (1999). The effect of epidermal growth factor on the preimplantation development, implantation and its receptor expression in mouse embryos. J Obstet Gynaecol Res *25*, 87-93.
Kim, E.J.Y., Anko, M.L., Flensberg, C., Majewski, I.J., Geng, F.S., Firas, J., Huang, D.C.S., van Delft, M.F., and Heath, J.K. (2018). BAK/BAX-Mediated Apoptosis Is a Myc-Induced Roadblock to Reprogramming. Stem Cell Reports *10*, 331-338.
Kopf, M., Baumann, H., Freer, G., Freudenberg, M., Lamers, M., Kishimoto, T., Zinkernagel, R., Bluethmann, H., and Kohler, G. (1994). Impaired immune and acute-phase responses in interleukin-6-deficient mice. Nature *368*, 339-342.
Kuilman, T., Michaloglou, C., Vredeveld, L.C., Douma, S., van Doorn, R., Desmet, C.J., Aarden, L.A., Mooi, W.J., and Peeper, D.S. (2008). Oncogene-induced senescence relayed by an interleukin-dependent inflammatory network. Cell *133*, 1019-1031.

Li, H., Collado, M., Villasante, A., Strati, K., Ortega, S., Canamero, M., Blasco, M.A., and Serrano, M. (2009). The Ink4/Arf locus is a barrier for iPS cell reprogramming. Nature *460*, 1136-1139.
Li, R., Liang, J., Ni, S., Zhou, T., Qing, X., Li, H., He, W., Chen, J., Li, F., Zhuang, Q., *et al*. (2010). A mesenchymal-to-epithelial transition initiates and is required for the nuclear reprogramming of mouse fibroblasts. Cell Stem Cell *7*, 51-63.
Liu, X., Sun, H., Qi, J., Wang, L., He, S., Liu, J., Feng, C., Chen, C., Li, W., Guo, Y., *et al*. (2013). Sequential introduction of reprogramming factors reveals a time-sensitive requirement for individual factors and a sequential EMT-MET mechanism for optimal reprogramming. Nat Cell Biol *15*, 829-838.
Mahmoudi, S., Mancini, E., Xu, L., Moore, A., Jahanbani, F., Hebestreit, K., Srinivasan, R., Li, X., Devarajan, K., Prelot, L., *et al*. (2019). Heterogeneity in old fibroblasts is linked to variability in reprogramming and wound healing. Nature *574*, 553-558.
Mai, T., Markov, G.J., Brady, J.J., Palla, A., Zeng, H., Sebastiano, V., and Blau, H.M. (2018). NKX3-1 is required for induced pluripotent stem cell reprogramming and can replace OCT4 in mouse and human iPSC induction. Nat Cell Biol *20*, 900-908.
Marion, R.M., Strati, K., Li, H., Tejera, A., Schoeftner, S., Ortega, S., Serrano, M., and Blasco, M.A. (2009). Telomeres acquire embryonic stem cell characteristics in induced pluripotent stem cells. Cell Stem Cell *4*, 141-154.
Mosteiro, L., Pantoja, C., Alcazar, N., Marion, R.M., Chondronasiou, D., Rovira, M., Fernandez-Marcos, P.J., Munoz-Martin, M., Blanco-Aparicio, C., Pastor, J., *et al*. (2016). Tissue damage and senescence provide critical signals for cellular reprogramming in vivo. Science *354*.
Mosteiro, L., Pantoja, C., de Martino, A., and Serrano, M. (2018). Senescence promotes in vivo reprogramming through p16(INK)(4a) and IL-6. Aging Cell *17*.
Munoz-Canoves, P., Scheele, C., Pedersen, B.K., and Serrano, A.L. (2013). Interleukin-6 myokine signaling in skeletal muscle: a double-edged sword? FEBS J *280*, 4131-4148.
Munoz-Espin, D., and Serrano, M. (2014). Cellular senescence: from physiology to pathology. Nat Rev Mol Cell Biol *15*, 482-496.
Ocampo, A., Reddy, P., Martinez-Redondo, P., Platero-Luengo, A., Hatanaka, F., Hishida, T., Li, M., Lam, D., Kurita, M., Beyret, E., *et al*. (2016). In Vivo Amelioration of Age-Associated Hallmarks by Partial Reprogramming. Cell *167*, 1719-1733 e1712.
Pommer, M., Kuphal, S., and Bosserhoff, A.K. (2021). Amphiregulin Regulates Melanocytic Senescence. Cells *10*.
Rhinn, M., Ritschka, B., and Keyes, W.M. (2019). Cellular senescence in development, regeneration and disease. Development *146*.
Ruiz, S., Panopoulos, A.D., Herrerias, A., Bissig, K.D., Lutz, M., Berggren, W.T., Verma, I.M., and Izpisua Belmonte, J.C. (2011). A high proliferation rate is required for cell reprogramming and maintenance of human embryonic stem cell identity. Curr Biol *21*, 45-52.
Samavarchi-Tehrani, P., Golipour, A., David, L., Sung, H.K., Beyer, T.A., Datti, A., Woltjen, K., Nagy, A., and Wrana, J.L. (2010). Functional genomics reveals a BMP-driven mesenchymal-to-epithelial transition in the initiation of somatic cell reprogramming. Cell Stem Cell *7*, 64-77.
Sancho-Martinez, I., and Izpisua Belmonte, J.C. (2013). Stem cells: Surf the waves of reprogramming. Nature *493*, 310-311.
Schuldiner, M., Yanuka, O., Itskovitz-Eldor, J., Melton, D.A., and Benvenisty, N. (2000). Effects of eight growth factors on the differentiation of cells derived from human embryonic stem cells. Proc Natl Acad Sci U S A *97*, 11307-11312.
Serrano, A.L., Baeza-Raja, B., Perdiguero, E., Jardi, M., and Munoz-Canoves, P. (2008). Interleukin-6 is an essential regulator of satellite cell-mediated skeletal muscle hypertrophy. Cell Metab *7*, 33-44.
Shiraha, H., Gupta, K., Drabik, K., and Wells, A. (2000). Aging fibroblasts present reduced epidermal growth factor (EGF) responsiveness due to preferential loss of EGF receptors. J Biol Chem *275*, 19343-19351.
Shoyab, M., McDonald, V.L., Bradley, J.G., and Todaro, G.J. (1988). Amphiregulin: a bifunctional growth-modulating glycoprotein produced by the phorbol 12-myristate 13-acetate-treated human breast adenocarcinoma cell line MCF-7. Proc Natl Acad Sci U S A *85*, 6528-6532.
Shoyab, M., Plowman, G.D., McDonald, V.L., Bradley, J.G., and Todaro, G.J. (1989). Structure and function of human amphiregulin: a member of the epidermal growth factor family. Science *243*, 1074-1076.

Thery, C., Amigorena, S., Raposo, G., and Clayton, A. (2006). Isolation and characterization of exosomes from cell culture supernatants and biological fluids. Curr Protoc Cell Biol *Chapter 3*, Unit 3 22.
Tran, K.T., Rusu, S.D., Satish, L., and Wells, A. (2003). Aging-related attenuation of EGF receptor signaling is mediated in part by increased protein tyrosine phosphatase activity. Exp Cell Res *289*, 359-367.
Utikal, J., Polo, J.M., Stadtfeld, M., Maherali, N., Kulalert, W., Walsh, R.M., Khalil, A., Rheinwald, J.G., and Hochedlinger, K. (2009). Immortalization eliminates a roadblock during cellular reprogramming into iPS cells. Nature *460*, 1145-1148.
Wang, Y.X., Feige, P., Brun, C.E., Hekmatnejad, B., Dumont, N.A., Renaud, J.M., Faulkes, S., Guindon, D.E., and Rudnicki, M.A. (2019). EGFR-Aurka Signaling Rescues Polarity and Regeneration Defects in Dystrophin-Deficient Muscle Stem Cells by Increasing Asymmetric Divisions. Cell Stem Cell *24*, 419-432 e416.
Wood, E.R., Truesdale, A.T., McDonald, O.B., Yuan, D., Hassell, A., Dickerson, S.H., Ellis, B., Pennisi, C., Horne, E., Lackey, K., *et al*. (2004). A unique structure for epidermal growth factor receptor bound to GW572016 (Lapatinib): relationships among protein conformation, inhibitor off-rate, and receptor activity in tumor cells. Cancer Res *64*, 6652-6659.
Xu, Q., Long, Q., Zhu, D., Fu, D., Zhang, B., Han, L., Qian, M., Guo, J., Xu, J., Cao, L., *et al*. (2019). Targeting amphiregulin (AREG) derived from senescent stromal cells diminishes cancer resistance and averts programmed cell death 1 ligand (PD-L1)-mediated immunosuppression. Aging Cell *18*, e13027.
Yoshida, Y., Takahashi, K., Okita, K., Ichisaka, T., and Yamanaka, S. (2009). Hypoxia enhances the generation of induced pluripotent stem cells. Cell Stem Cell *5*, 237-241.
Yu, M., Wei, Y., Xu, K., Liu, S., Ma, L., Pei, Y., Hu, Y., Liu, Z., Zhang, X., Wang, B., *et al*. (2019). EGFR deficiency leads to impaired self-renewal and pluripotency of mouse embryonic stem cells. PeerJ *7*, e6314.
Yun, M.H., Davaapil, H., and Brockes, J.P. (2015). Recurrent turnover of senescent cells during regeneration of a complex structure. Elife *4*.
Zaiss, D.M.W., Gause, W.C., Osborne, L.C., and Artis, D. (2015). Emerging functions of amphiregulin in orchestrating immunity, inflammation, and tissue repair. Immunity *42*, 216-226.
Zhang, C., Li, Y., Wu, Y., Wang, L., Wang, X., and Du, J. (2013). Interleukin-6/signal transducer and activator of transcription 3 (STAT3) pathway is essential for macrophage infiltration and myoblast proliferation during muscle regeneration. J Biol Chem *288*, 1489-1499.

FIGURE LEGEND

Figure 1. Senescence promotes *in vitro* reprogramming in a stress-dependent manner

A. Scheme of the experiments. **B & C.** Relative *in vitro* reprogramming efficiency of i4F MEFs exposed to secretome of non-senescent compared to senescent cells generated by different stress (corresponding to the respective controls: RS and IRIS to non-sen and OIS to vector alone). RS: replicative senescence, IRIS : γ-irradiation, OIS: oncogene-induced senescence. **B.** Co-culture system; Representative image of plate stained with alkaline phosphatase (AP) to reveal colonies arising from reprogramming (right panel). **C.** Conditioned medium system (CM). **D.** Reprogramming fold change of i4F MEFs cultured in different duration of OIS-CM before switching to Ctrl-CM. Scheme of the experiment (left panel). All the reprogramming fold changes was normalized to i4F in Ctrl-CM for 12 days, indicated by the blue

dash line. Data correspond to the average ± s.d. using indicated n number of independent experiments. Statistical significance was assessed by ordinary one-way ANOVA test: *p < 0.05; **p < 0.01; **** p < 0.0001. See also **Figure S1**.

Figure 2. *in vivo* reprogramming in the skeletal muscle occurs normally in *Il6*$^{-/-}$ mice

A. Relative reprogramming efficiency of the i4F MEFs cultured in the CM derived from either WT or *Il6*$^{-/-}$ senescent cells. Senescence was induced using two different stresses, IRIS and OIS. Fold change was normalized with CM derived of respective non-senescent counterparts. **B.** Reprogramming efficiency of i4F MEFs cultured in CM of WT or *Il6*$^{-/-}$ senescent cells compared to treatment of IL-6 blocking antibody. Senescence was induced by over-expression of oncogene (OIS). Data correspond to the average ± s.d. using indicated n number of independent experiments. **C.** Transverse TA cryosections of indicated genotypes and sex after histological staining with Haematoxylin and Eosin (H&E). Dashed circle highlights dysplasia region. Scale bar: 50 μm. **D.** Experimental scheme (Upper panel) and quantification of **C.** The value represents one TA per mouse. Statistical significance was assessed by ordinary one-way ANOVA test: *p < 0.05; **p < 0.01; ***p < 0.001. See also **Figure S2.**

Figure 3. Proteomic analysis of oncogenic stress-induced secretome in *Il6*$^{-/-}$ MEFs

A. Fold change of reprogramming efficiency of i4F MEFs cultured in indicated different combination of various fractions of CM from non-senescent (Ctrl) or senescent (OIS) *Il6*$^{-/-}$. SN: supernatants (soluble proteins); sEV: small extracellular vesicles (exosome). Reprogramming efficiency fold change normalized to Ctrl-CM. Data correspond to the average ± s.d. using indicated n number of independent experiments. **B.** Volcano plot shows $\log_2$ fold change in protein intensity against the -log10 pvalue in SEN compared to Ctrl; blue dots are proteins with significant differential expression (FDR< 0.01). **C.** Summary of proteins either with significantly altered secretion (q-value < 0.01 and >2-fold change) by senescent (SEN) compared with quiescent cells (Ctrl), or exclusively detected in all repeats from one condition, following oncogenic stress (OIS) in senescent *Il6*$^{-/-}$ primary MEFs. **D.** ClueGO (Bindea et al., 2009) pathway enrichment and network analyses of OIS-secretome. Pathways of the same color have

⩾50% similarity. Connecting lines represent Kappa connectivity scores > 40%. Statistical significance was assessed by ordinary one-way ANOVA test: **p < 0.01. See also **Figure S3.**

Figure 4. AREG promotes *in vitro* reprogramming

A. Experimental scheme (upper panel). Fold change of reprogramming efficiency of i4F MEFs with different dosages of recombinant AREG protein. Normalized to Vehicle control (PBS). Representative image of plate stained with alkaline phosphatase (AP) to reveal colonies arising from reprogramming (right panel). **B.** Experimental scheme (upper panel). Comparison of reprogramming efficiency between PBS and recombinant AREG after different duration of DOX treatment. Data correspond to the average ± s.d. using indicated n number of independent experiments. **C-E.** Kinetics of expression of indicated genes at the indicated days during reprogramming comparing between PBS and AREG as measured by quantitative RT-PCR. Data correspond to the average ± s.e.m. of at least 2 independent assays. For each assay, qRT-PCR values were obtained in duplicate. Statistical significance was assessed by ordinary one-way ANOVA test for **A**, and two-way ANOVA test for **B-E:** *p < 0.05; **p < 0.01; ***p < 0.001. See also **Figure S4.**

Figure 5. AREG promotes *in vivo* reprogramming

A. Relative reprogramming efficiency of i4F MEFs treated with EGF (100ng/mL). Relative to PBS treated sample. **B.** Relative reprogramming efficiency of i4F MEFs with indicated treatment. Relative to PBS treated sample. Data correspond to the average ± s.d. of using indicated n number of different experiments using i4F MEFs generated from different embryos (A & B). **C.** Reprogramming efficiency of dermal fibroblasts derived from i4F mice with the indicated treatment and age. Data correspond to the average ± s.d. of using indicated n number of different MDF isolates. **D.** Experimental scheme for AREG administration during *in vivo* reprogramming. **E.** Representative TA sections with immunohistochemistry staining of anti-Nanog and histological staining of SAβGal of indicated treatment. Scale bar: 50 μm. **F.** Quantification of E. Data correspond to the average ± s.d. of using indicated n number of different mouse (average of two TA per mouse). Statistical significance was

assessed by the Mann-Whitney test (A) and ordinary one-way ANOVA (B, C, and F): *p < 0.05; **p < 0.01; ***p < 0.001. See also **Figure S5.**

Figure 1. Senescence promotes *in vitro* reprogramming in a stress-dependent manner

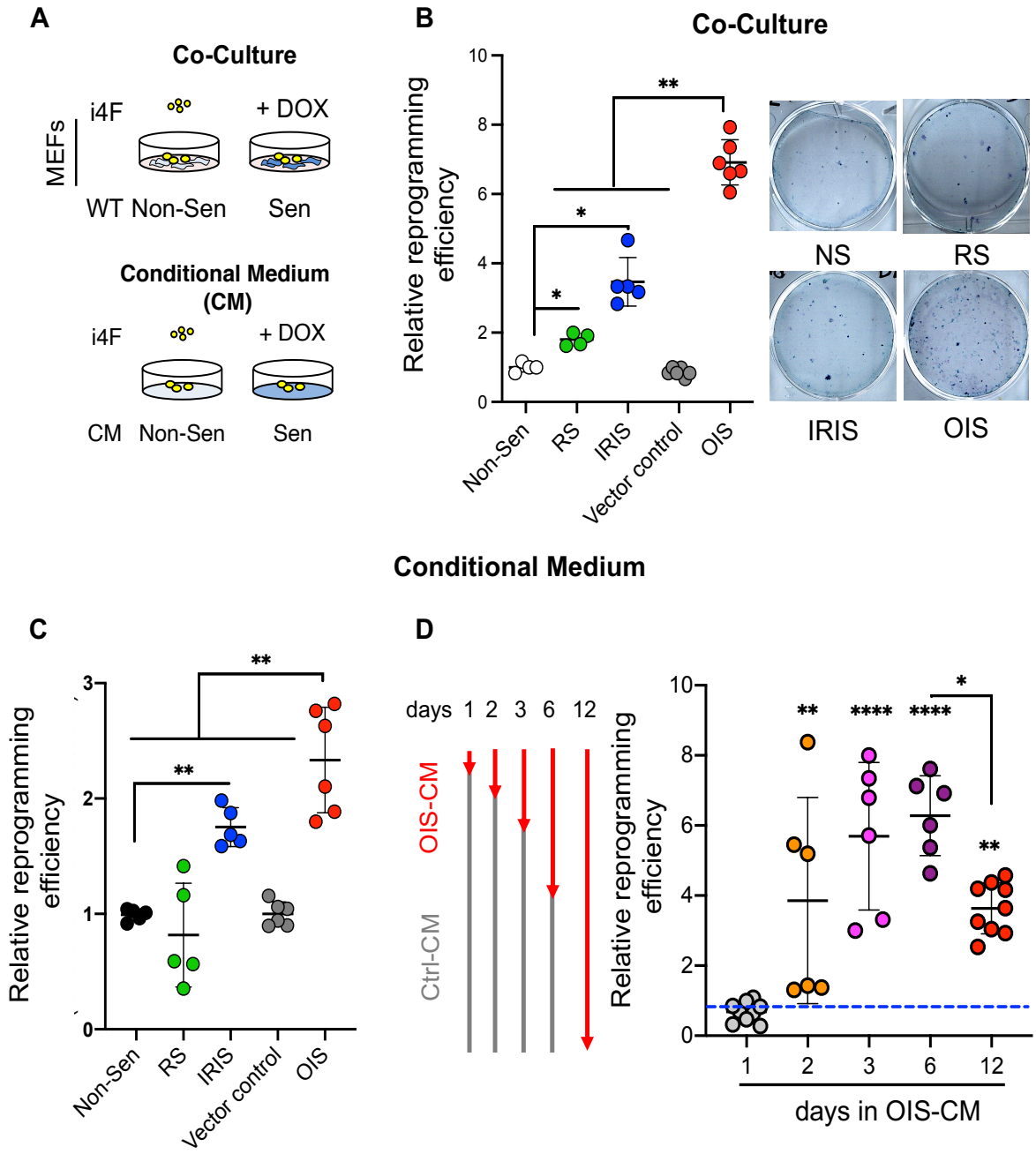

Figure 2. ***in vivo*** **reprogramming in the skeletal muscle occurs normally in** ***Il6*** $^{-/-}$ **mice**

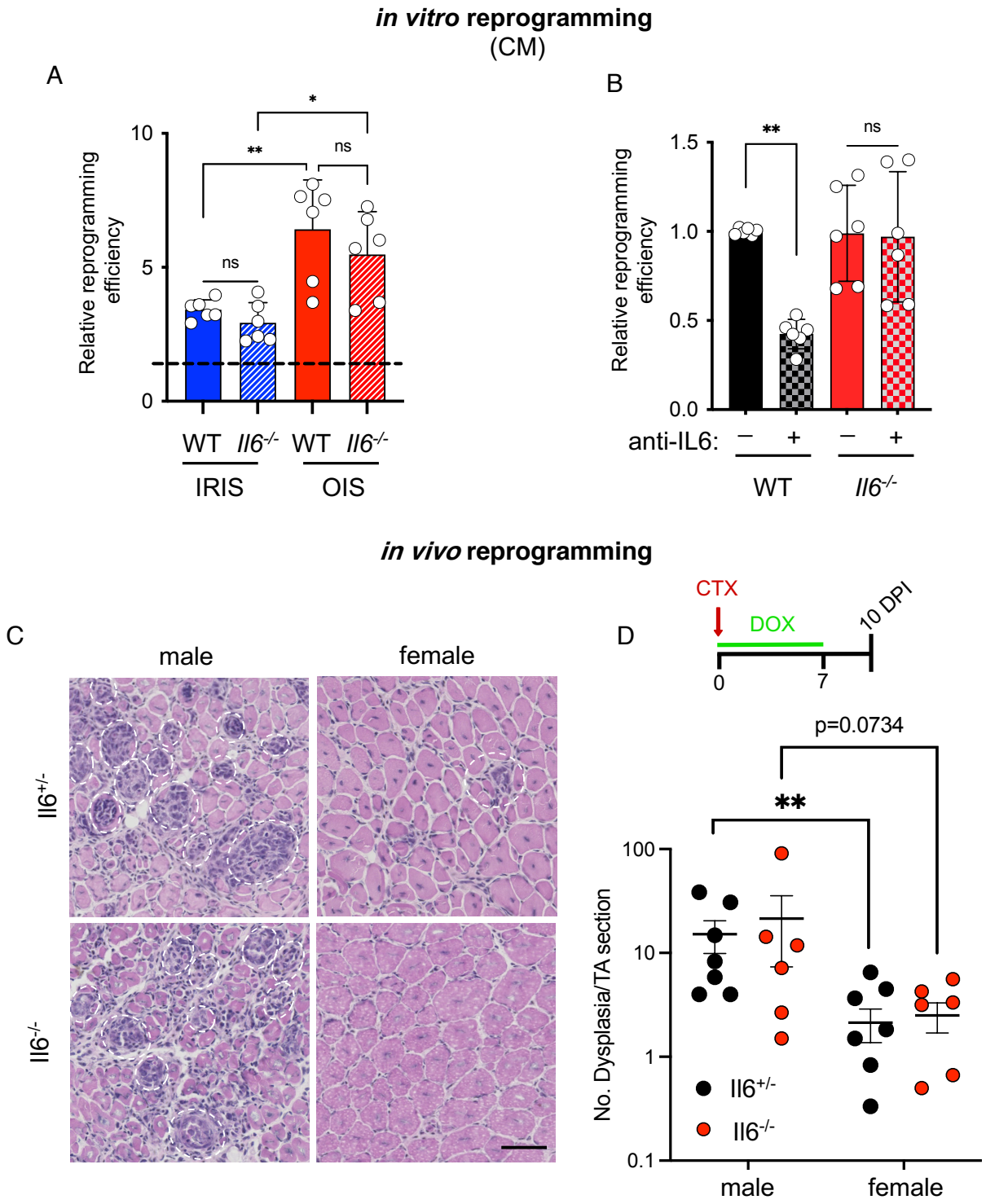

Figure 3. Proteomic analysis of oncogenic stress-induced secretome in *Il6*$^{-/-}$ MEFs

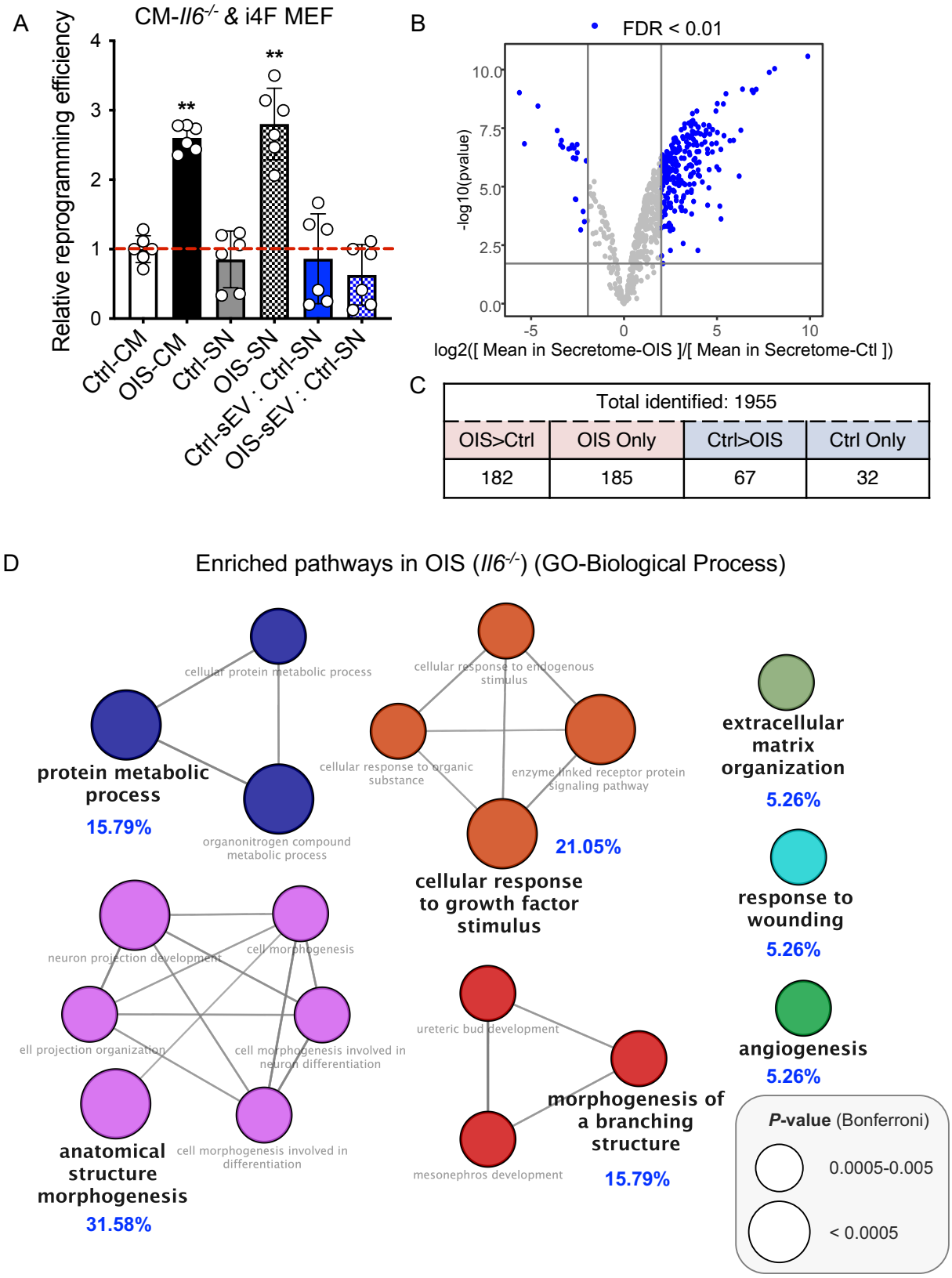

Total identified: 1955			
OIS>Ctrl	OIS Only	Ctrl>OIS	Ctrl Only
182	185	67	32

Figure 4. AREG promotes *in vitro* reprogramming

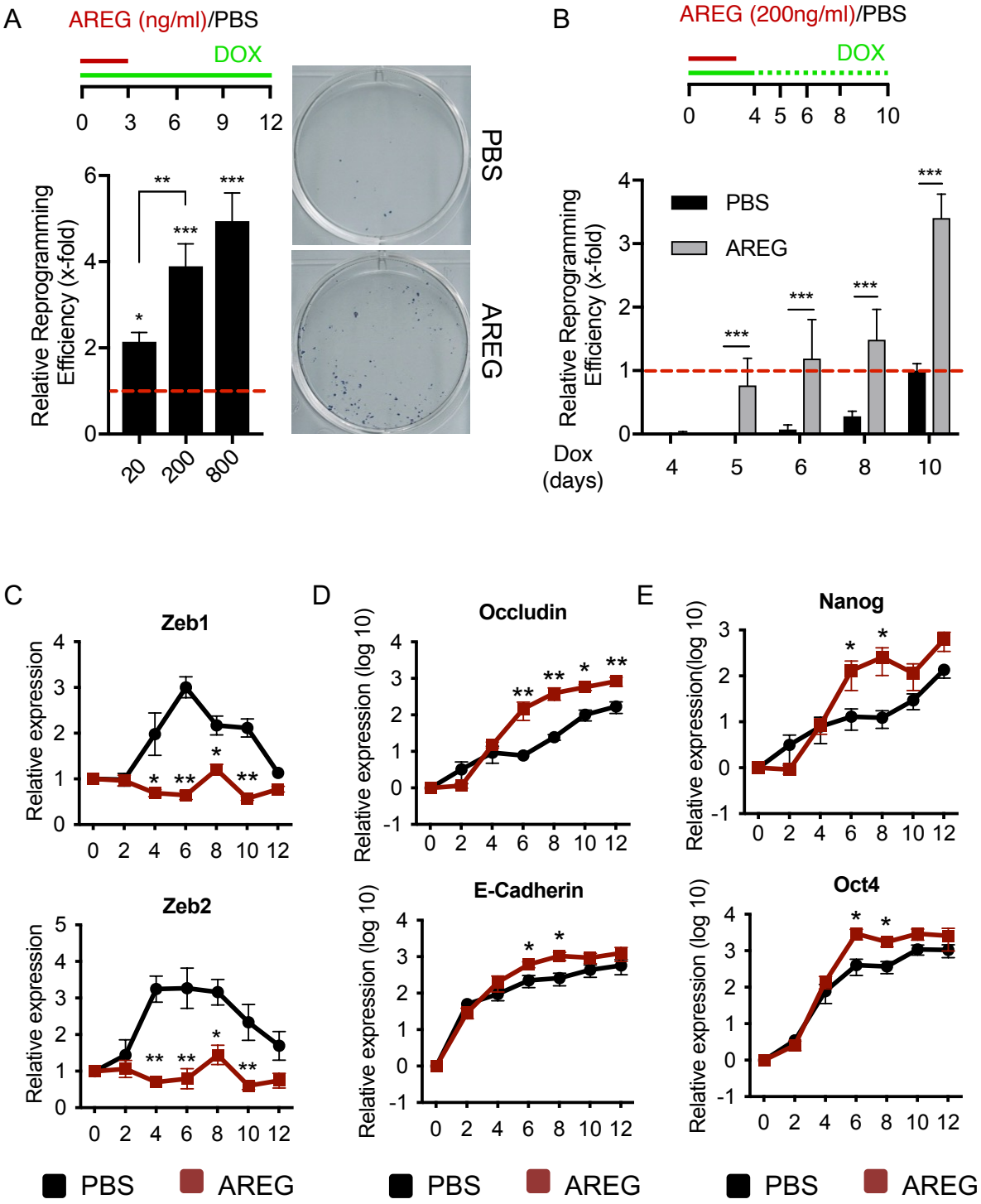
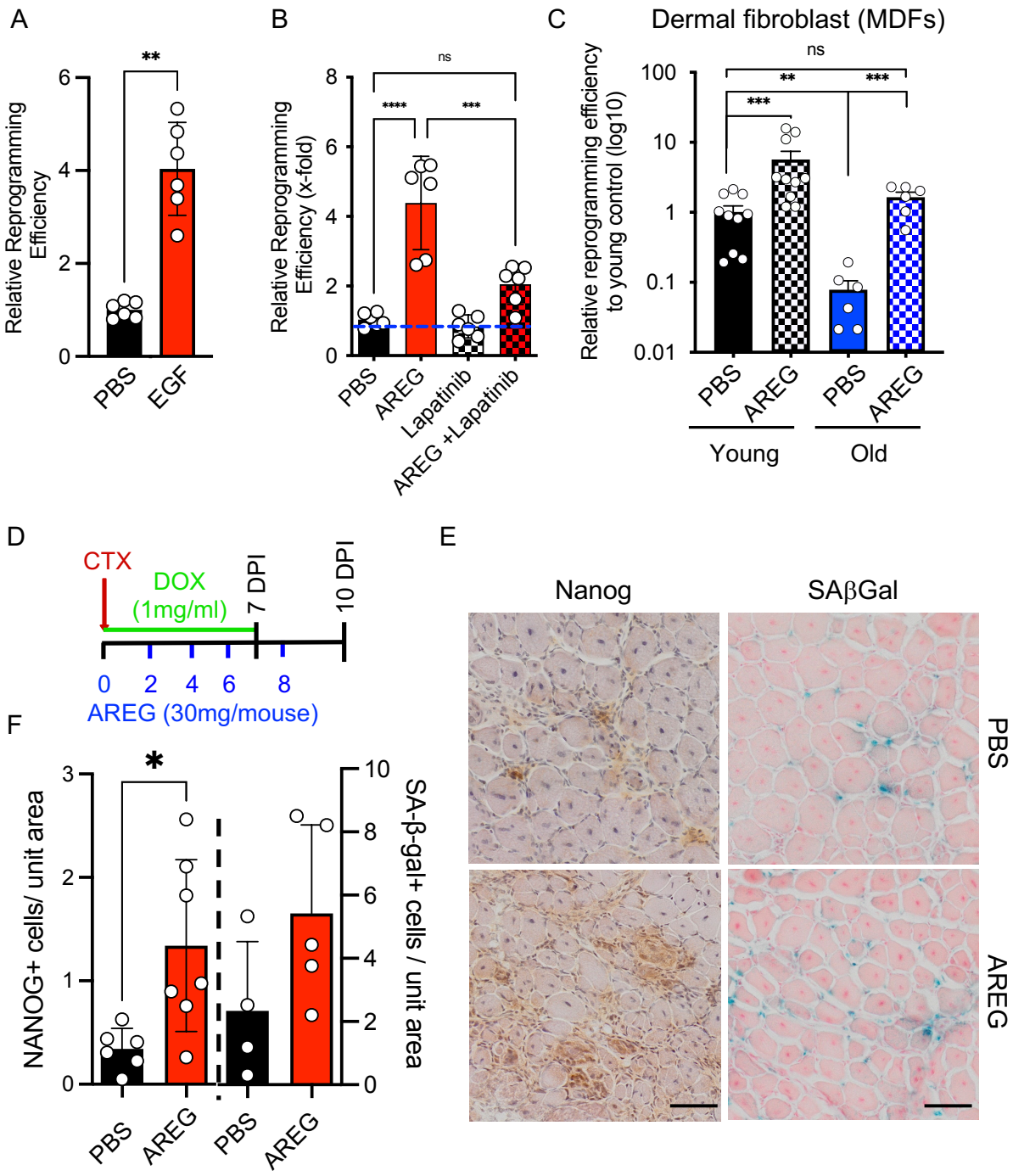
Figure 5. AREG promotes *in vivo* reprogramming